ELSEVIER

European Journal of Cancer 40 (2004) 1554–1565

European Journal of Cancer

www.ejconline.com

In vivo and *in vitro* evaluation of erianin, a novel anti-angiogenic agent

Y.-Q. Gong [a,b], Y. Fan [a], D.-Z. Wu [a], H. Yang [b], Z.-B. Hu [a], Z.-T. Wang [a,b,*]

[a] *Institute of Chinese Materia Medica, Shanghai University of Traditional Chinese Medicine, 1200 Cailun Road, Zhangjiang Hi-Tech Park, Shanghai 201203, PR China*

[b] *Department of Pharmacognosy, China Pharmaceutical University, Nanjing 210038, PR China*

Received 11 December 2003; accepted 12 January 2004
Available online 25 May 2004

Abstract

This study evaluated the anti-angiogenic activities of erianin *in vivo* and *in vitro*. Erianin, a natural product from *Dendrobium chrysotoxum*, caused moderate growth delay in xenografted human hepatoma Bel7402 and melanoma A375 and induced significant vascular shutdown within 4 h of administering 100 mg/kg of the drug. Erianin also displayed potent anti-angiogenic activities *in vitro*: it abrogated spontaneous or basic fibroblast growth factor-induced neovascularisation in chick embryo; it inhibited proliferation of human umbilical vein endothelial cells (EC_{50} 34.1 ± 12.7 nM), disrupted endothelial tube formation, and abolished migration across collagen and adhesion to fibronectin. Erianin also exerted selective inhibition toward endothelial cells, and quiescent endothelium showed more resistance than in proliferative and tumour conditions. In a cytoskeletal study, erianin depolymerised both F-actin and β-tubulin, more significantly in proliferating endothelial cells than in confluent cells. In conclusion, erianin caused extensive tumour necrosis, growth delay and rapid vascular shutdown in hepatoma and melanoma models; it inhibited angiogenesis *in vivo* and *in vitro* and induced endothelial cytoskeletal disorganisation. These findings suggest that erianin has the therapeutic potential to inhibit angiogenesis *in vivo* and *in vitro*.

Keywords: Erianin; Anti-angiogenesis; Human umbilical vein endothelial cells; Hepatoma Bel7402; Melanoma A375; *Dendrobium chrysotoxum*

1. Introduction

Angiogenesis is critical to the survival and continued growth of a solid tumour mass and its metastases [1,2]. Tumour endothelium is therefore an important target for the development of new approaches to therapy [3]. Some anti-angiogenic agents, such as fumagillin [4], angiostatin [5], endostatin [6], neovastat [7], and combretastatin A-4 [8], have become the focus of new drug development.

Erianin (2-methoxy-5-[2-(3,4,5-trimethoxy-phenyl)-ethyl]-phenol) is a low molecular-weight natural product isolated from *Dendrobium chrysotoxum* Lindl., which is often used as an anti-pyretic and an analgesic in traditional Chinese medicine. Structurally, erianin contains two phenyl rings linked by a 2-carbon bridge with several methoxyl substitutions on the phenyl rings (Fig. 1) and belongs to the bibenzyl derivatives, in which many compounds have shown anti-viral [9], anti-bacterial [10], and anti-prostatic [11] activities. Structurally similar to erianin, some stilbene [12] and phenanthrene derivatives [13] display potent anti-tumour activity; combretastatin A-4 is a promising candidate for controlling the aberrant angiogenesis of tumour development.

In previous studies, we and others have found that erianin is active, with growth inhibitory effects on tumours *in vivo* and *in vitro* [14,15] and with apoptosis-inducing effects on carcinoma cells [16]. We have also recently demonstrated that erianin induces a JNK/SAPK-dependent metabolic inhibition in human umbilical vein endothelial cells (HUVECs) [17]. However, whether erianin's anti-tumour effect on solid tumours involves

* Corresponding author. Tel.: +86-21-51322507; fax: +86-21-51322519.
E-mail addresses: wangzht@shutcm.com, wangzht@hotmail.com (Z.-T. Wang).

0959-8049/$ - see front matter © 2003 Elsevier Ltd. All rights reserved.
doi:10.1016/j.ejca.2004.01.041

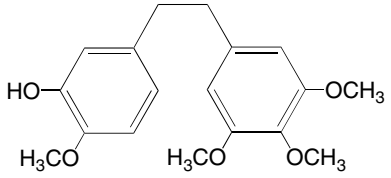

Fig. 1. Chemical structure of erianin.

anti-angiogenesis and what are the underlying cellular or molecular mechanisms remain to be discovered.

The aim of present study was to extend the previous observation on the anti-tumour activity of erianin and to evaluate its anti-angiogenic activity with *in vivo* and *in vitro* models. Experimental data presented here show that erianin displayed potent anti-angiogenic activity *in vivo* and *in vitro,* and inhibited proliferation in endothelial cells with high selectivity, and caused a cytoskeletal disturbance restricted to proliferating endothelium.

2. Materials and methods

2.1. Reagents and cell lines

Erianin was isolated from *D. chrysotoxum* Lindl. [18], identified by several conventional methods, with a purity of 98%. Basic fibroblast growth factor (bFGF), calf skin or rat rail collagen type I, crystal violet, endothelial cell growth supplements (ECGS), fibronectin, fluorescein isothiocyanate (FITC)–phalloidin, Hoechst-33342, and 3-(4,5-dimethylthiazol-2-yl)-2,5-diphenyltetrazolium bromide (MTT) were obtained from Sigma (St. Louis, MO). Mouse monoclonal antibody to CD31 was purchased from NeoMarkers (Fremont, CA) and FITC-conjugated mouse monoclonal antibody to β-tubulin from Sigma. Human hepatoma Bel7402 cells were kindly provided by Dr. Ren Xu (Institute of Biochemistry and Cell Biology, Shanghai Institutes for Biological Sciences, Chinese Academy of Sciences). Mouse fibroblast NIH/3T3 cells and human melanoma A375 cells were obtained from the Cell Bank of the Chinese Academy of Sciences (Shanghai, PR China). Unless otherwise mentioned, reagents for cell culture were purchased from Gibco/Invitrogen (Grand Island, NY) and biochemical reagents were obtained from Sigma or Ameresco (Solon, OH).

2.2. Tumour transplantation and drug administration

Female BALB/c mice aged 8 weeks (Shanghai Cancer Institute, Shanghai, PR China) were housed in barrier facilities with food and water *ad libitum*. Tumour cell suspensions with density of about 10^8 cells/ml in phosphate-buffered saline (PBS), pH 7.4, were prepared from the tumour tissue derived from subcutaneous transplantation of Bel7402 and A375 cells. After the implantation in nude mice of 5 μl/g tumour cell suspensions, animals were randomly divided into four groups as follows: vehicle group [2 ml/kg dimethyl sulphoxide (DMSO)], drug treatment groups [100 mg/kg erianin (50 mg/ml in DMSO) and 50 mg/kg erianin (25 mg/ml in DMSO)], and a control group for histological assessment and a vascular shutdown study (non-treatment). All agents were administered intraperitoneally in mice at 20 μl/10 g body weight once tumours had reached minimum diameters of 4×5 mm (approximately days 7 after tumour implantation). Every 3 or 4 days, tumours were measured by calipers in two perpendicular diameters and their volume estimated using the formula: $V = 0.52 \times L^2 \times W$ (V, volume; L, length; and W, width) [19]. Semi-log plots of relative tumour volume against time were made and the time taken for tumour doubling to occur was recorded. At day 20, mice were killed and the tumours weighed.

2.3. Histological assessment and immunohistochemistry

Tumours were collected and fixed in Bouin fixative for 24 h. After dehydration and embedding in paraffin, tumour tissues were sectioned at 8 μm for histological assessment and immunohistochemistry. A minimum of five sections stained with haematoxylin and eosin (H&E) from each tumour were selected for evaluating the extent of necrosis, which was quantified: percentage necrosis was with the image-analysis program *Image-Pro plus* (Media Cybernetics, Silver Spring, MD). Other tissue sections were rehydrated and unmasked with treatment with 1 mM EDTA (pH 8.0) at 95 °C for 10 min. Immunohistochemistry was performed according to the instructions for the UltraVision Detection DAB system (LabVision, Fremont, CA) with a monoclonal antibody to CD31/PECAM at 1:50 dilution for 30 min at room temperature. As a negative control, the primary antibody was omitted. Positive immunostaining, which appeared as a brown colour, was visualised under a BX51 microscope with a DP50 colour CCD (Olympus, Tokyo, Japan), and intratumoural microvessel density (IMD) was assayed with the *Image-Proplus* software.

2.4. Vascular fluorescent perfusion

Hoechst-33342 was used as a marker for vascular spaces in tumours [20]. After a 1-min exposure to 40 mg/kg Hoechst-33342 (given intravenously in sterile saline), the mice were killed by cervical dislocation and the tumours resected. Tumours were wrapped in OCT compound (Sakura Finetek, Torrance, CA) and immediately immersed in liquid nitrogen for subsequent frozen sectioning. Frozen sections (6 μm) were cut on a cryostat at three different levels between one pole and the equatorial plane, and viewed in a light microscope

under ultraviolet illumination. Perfusion was observed as fluorescence and counts made, in which squares containing fluorescence were counted as positive, with the image-analysis procedure described above. A minimum of five sections per tissue was examined and five fields counted per section to detect the vascular volume. Results were analysed with the *Image-Pro plus* software.

2.5. Angiogenesis assay on chick chorioallantoic membrane

The ability of erianin to inhibit angiogenesis *in vivo* was evaluated by chick embryo chorioallantoic membrane (CAM) assay, as previously described, with minor modifications [21]. In brief, fertilised chicken eggs were incubated at 37 °C at constant humidity. On incubation day 3, a square window was opened in the shell and 2–3 ml albumen was removed to allow detachment of the developing CAM, and the window was then sealed with glass. On day 8 of development, blank filter discs (5 mm diameter) and discs containing 250 ng bFGF, bFGF plus 2 or 10 μg erianin (dissolved in ethanol, which was later evaporated off), or erianin alone (2, 10 or 50 μg) were placed on the top of growing CAMs under sterile conditions. The zone around the methylcellulose disc was observed macroscopically 48 h after disc placement, and all blood vessels within a 100-mm^2 area surrounding the applied disc were traced and analysed at 50× magnification.

2.6. Cell culture

HUVECs were isolated, cultured, and characterised with von Willebrand factor, as described previously [22]. To achieve confluence, HUVECs were cultured in gelatin-coated culture flasks in a moist atmosphere (5% CO_2–95% air) at 37 °C in Dulbecco's modified Eagle's medium (DMEM) supplemented with 2 mM L-glutamine, 20 mM Hepes, 10% fetal bovine serum (FBS), 50 μg/ml ECGS, 5 U/ml heparin, 100 IU/ml penicillin, and 100 μg/ml streptomycin. Confluent cells were used between the second and the sixth passages. Bel7402 and A375 cells were maintained in DMEM medium supplemented with 10% FBS. Tumour-conditioned medium was collected from a DMEM medium subjected to confluent A375 tumour cells for 24 h, then centrifuged at 10,000*g* for 30 min at 4 °C, filter sterilised (0.22 μm), and supplemented with the reagents for endothelial cell culture as above (pH 7.4).

2.7. Cell-proliferation assays

Cell proliferation was determined by standard MTT assay in normal, tumour-conditioned HUVECs, and NIH/3T3 and A375 cells [23]. Erianin was dissolved in DMSO and diluted in DMEM medium (the concentration of DMSO did not exceed 0.1% v/v). Cells were incubated in their complete medium containing 10% FBS (positive control), the complete medium plus erianin, or the starvation medium without FBS (negative control). Cell proliferation was evaluated following a continuous 48-h exposure to a range of drug concentrations. To assess the effect on quiescent HUVECs, erianin was not introduced until the cells on the microplate had reached confluence. Absorbance at 540 nm was determined using a Spectramax 390 microplate reader (Molecular Devices, Sunnyvale, CA). Each sample was assayed in eight duplicates and each assay was repeated at least four times. The experimental data were normalised for comparison as the percentage of positive control. In addition, to validate the non-cytotoxic concentration, a lactate dehydrogenase (LDH) assay with a commercial kit (Sigma) was performed by 24-h incubation of HUVECs with erianin at that concentration [24]. The results on releasing LDH were expressed as the percentage of the total LDH present in the culture (releasing + intracellular), as we reported previously [25].

2.8. Endothelial tube formation

The tube-formation assay was performed according to a modified method [26]. In brief, three-dimensional collagen gel was prepared in 24-well plates by the addition of chilled 500 μl rat rail collagen type I solution (1.1 mg/ml) to each well, adjusted to neutral pH with $NaHCO_3$ and allowed to polymerise for 20 min at 37 °C. HUVECs harvested using trypsin/EDTA were seeded at a density of 5×10^4 cells per well on the polymerised collagen and allowed to attach for 24 h. The plate was incubated in the presence or absence of 10 nM erianin at 37 °C for 24 h, and some of the control with tube formation was further subjected to 10 nM erianin exposure for various time intervals. The medium was aspirated and cells were fixed with 3.7% formalin in PBS. Representative photographs were taken using a CK40 microscope (Olympus).

2.9. HUVEC-migration assay

The ability of HUVEC to migrate through collagen was examined using 6-well Transwell chambers (Costar, Corning, NY) [27]. The filter membrane (8 μm pore) of the Transwell was coated with 1.1 mg/ml type I calf-skin collagen solution at 37 °C for 60 min. The cultured HUVECs were starved for 2 h in DMEM medium containing 0.5% FBS and then subcultured to Transwells at a density of 2×10^5 cells/well. After 2-h incubation for cell attachment, the same medium alone, or with 10 ng/ml bFGF as a chemotactant, or bFGF plus erianin (10 or 100 nM) was added in the lower chamber. Following 24-h incubation at 37 °C, the Transwells were removed and the cells on the upper side of the filter were scraped off. Remand cells migrating to the lower side

were fixed in methanol and stained with Wright's dye solution. Migration was calculated as the average number of cells observed in five random fields (100×) at least in five wells, and results were analysed with the *Image-Pro plus* software.

2.10. Cell-adhesion assay

After 96-well plates were coated with a fibronectin solution (20 μg/ml) at 4 °C overnight, HUVECs were plated (5×10^3 cells/well) in starvation medium alone or containing 10 or 100 nM erianin for 90 min at 37 °C, and then non-adhesive cells were washed off, as previously described [28]. The remaining adhesive cells were fixed for 15 min at room temperature with 2.5% glutaraldehyde and stained with 0.1% crystal violet in 20% methanol for 20 min, solubilised with 10% acetate, and read at 595 nm in a microplate reader. The cell number was derived from a calibration curve set up with a known number of cells.

2.11. Cytoskeletal immunofluorescence

Cytoskeletal visualisation was achieved using FITC–phalloidin and FITC–antibody to β-tubulin [29]. The control or erianin-treated HUVECs, A375, Bel7402, and NIH/3T3 cells on gelatin-coated glass coverslips (Bland, Germany) were fixed with 3.7% formalin for 15 min, permeabilised with 0.1% Triton X-100 for 5 min, and incubated with 50 μg/ml FITC–phalloidin or 1:25 dilution FITC–antibody to β-tubulin for 40 min at room temperature in a humid atmosphere. After thorough washing, coverslips were mounted with 80% glycerol in PBS and examined with an Axioskop-2 fluorescent microscope (Zeiss, Germany) equipped with an ISIS system cool-CCD (Zeiss).

2.12. Electron microscopy

HUVEC at 80–90% confluence were maintained for 1 h in DMEM supplemented with 10% FBS in the presence or absence of 10 nM erianin. The cells were then washed by PBS and fixed in 3% glutaraldehyde for 3 h, washed for 12 h, and post-fixed in 1% osmium tetroxide [28]. Afterwards, the cells were scraped off with a rubber bar, dehydrated in graded ethanols, and embedded in Epon 812. Ultrathin sections were cut with a diamond knife, stained with uranyl acetate followed by lead citrate, and examined in a Tecnai 12 transmission electron microscope (Philips, Holland).

2.13. Statistical analysis

All data were expressed as means ± SEM. Statistical significance was assessed by Mann–Whitney *U* analysis or Student's *t*-test with computer software *SigmaStat 2.0* (SPSS, Chicago, IL), and a *P*-value of less than 0.05 was accepted as a significant difference.

3. Results

3.1. 14-Day administration of erianin causes tumour growth delay

The ability of erianin to delay tumour growth was evaluated in human hepatoma Bel7402 and melanoma A375. Treatment of mice bearing these tumours with erianin (100 mg/kg per day intraperitoneal) resulted in a moderate delay, as indicated by increases in the mean time to tumour volume doubling (TVD); only slight and statistically insignificant effects were observed at 50 mg/kg/day (Table 1). Moreover, treatment with erianin at both doses induced manifest decreases in the ultimate weight of A375 tumours, but only erianin at 100 mg/kg per day caused significant inhibition of Bel7402 tumour weight (Table 1).

3.2. Acute treatment of erianin induces haemorrhagic necrosis and vascular shutdown in vivo

Morphological assessments were made in relation to acute treatment with erianin within 24 h in xenograft Bel7402 and A375 tumours. As vehicle controls, A375 tumours treated with 2 ml/kg DMSO showed their usual histological appearance of poor differentiation and

Table 1
In vivo evaluation of erianin against Bel7402 and A375 tumours

Tumours	Dose (mg/kg)	Median time to tumour volume doubling (days)	Growth delay (days)	Tumour weight (g)
Bel7402	Vehicle	4.62 ± 0.42		0.93 ± 0.12
	50	4.85 ± 0.71	0.23	0.67 ± 0.12
	100	5.81 ± 0.49*	1.19	0.55 ± 0.17*
A375	Vehicle	3.27 ± 0.35		1.80± 0.12
	50	3.61 ± 0.57	0.34	1.35 ± 0.14*
	100	5.86 ± 0.49*	1.59	0.82 ± 0.03**

*$P < 0.05$ and **$P < 0.01$, the statistical significance of anti-tumour effects was determined by Mann–Whitney *U* analysis comparing doubling time in vehicle vs. treated tumours.

Each value represents mean ± SEM ($n = 5$–6).

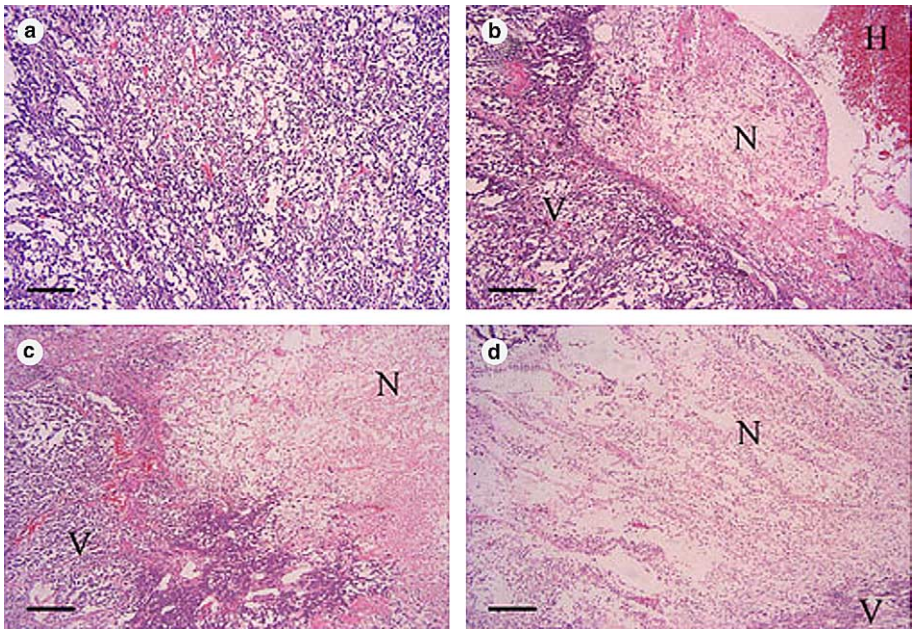

Fig. 2. Effect of erianin treatment on tissue morphology in A375 tumours. Xenograft tumours treated with dimethyl sulphoxide or 100 mg/kg erianin intraperitoneally over 24 h; tumour sections stained with H&E. (a) vehicle, no discernible necrosis; (b) 2-h treatment, haemorrhagic necrosis with obvious dividing line between viable and necrotic tissues; (c) 4-h treatment, massive necrosis; (d) 24-h treatment, extensive necrosis. N, necrosis; V, viable tumour; H, haemorrhage. Representative images taken from two independent experiments ($n = 4$–5 for each experiment). Bar = 50 μM.

limited necrosis (Fig. 2(a)). In contrast, 4- and 24-h treatment with 100 mg/kg erianin induced obvious haemorrhagic necrosis to different extents in A375 tumours (Fig. 2(c) and (d)), with necrotic areas of $52.4\% \pm 9.8\%$ and $84.3\% \pm 11.9\%$, respectively, and 2-h treatment caused local and limited necrosis but accompanied with manifest haemorrhage (Fig. 2(b)). Similar effects occurred in treated Bel7402 tumours (data not shown).

Vascular shutdown was studied with a combination of IMD and vascular volume assays, using CD31 immunohistochemistry and Hoechst-33342 perfusion, respectively. There was an abundant vascular distribution

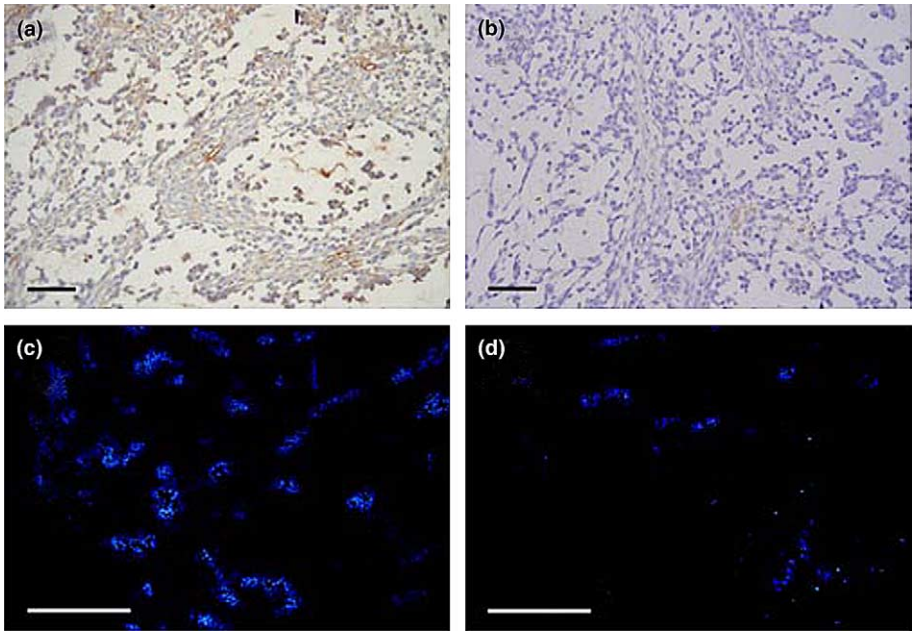

Fig. 3. Effect of erianin on vascular density and volume in A375 tumours. After treatment with dimethyl sulphoxide or 100 mg/kg erianin intraperitoneally, some tumours were fixed and used for vascular staining by CD31 immunohistochemistry: (a) vehicle; (b) erianin treatment for 4 h. Other tumours perfused with H33342 were sectioned for fluorescent microscopy: (c) frozen section of vehicle tumour; (d) treatment with erianin for 4 h. Images representative of separate triplicate assays ($n = 4$–6 for each experiment). Bar = 50 μM.

in A375 tumours (Fig. 3(a)), and 4-h treatment with 100 mg/kg erianin resulted in dramatic vascular shutdown and damage (Fig. 3(b)), with a decreased IMD of 22.7 ± 6.8 pixels per 100× field (176.8 ± 42.6 for vehicle tumour IMD). Similar results were obtained in Bel7402 tumours, as indicated by the IMD of 11.5 ± 1.7 after erianin treatment (127.7 ± 18.7 for vehicle IMD). The vascular volumes for 4-h 2 ml/kg DMSO-treated Bel7402 and A375 tumours (vehicle) were $6.9\% \pm 1.3\%$ and $8.7\% \pm 1.7\%$ as determined by image analysis in a fluorescent-perfusion assay [20], and in all 100 mg/kg drug-treated tumours very limited and only peripheral fluorescence could be seen (Fig. 3(c) and (d)).

3.3. Erianin inhibits CAM angiogenesis in vivo

Physiological angiogenesis was observed around the blank methylcellulose discs in CAM as a few surrounding vessels (Fig. 4(a)), whereas the discs absorbed with 250 ng bFGF induced a vasoproliferative response, allantoic vessels developed radially toward the discs in a spoked pattern (Fig. 4(b)). Meanwhile, erianin induced

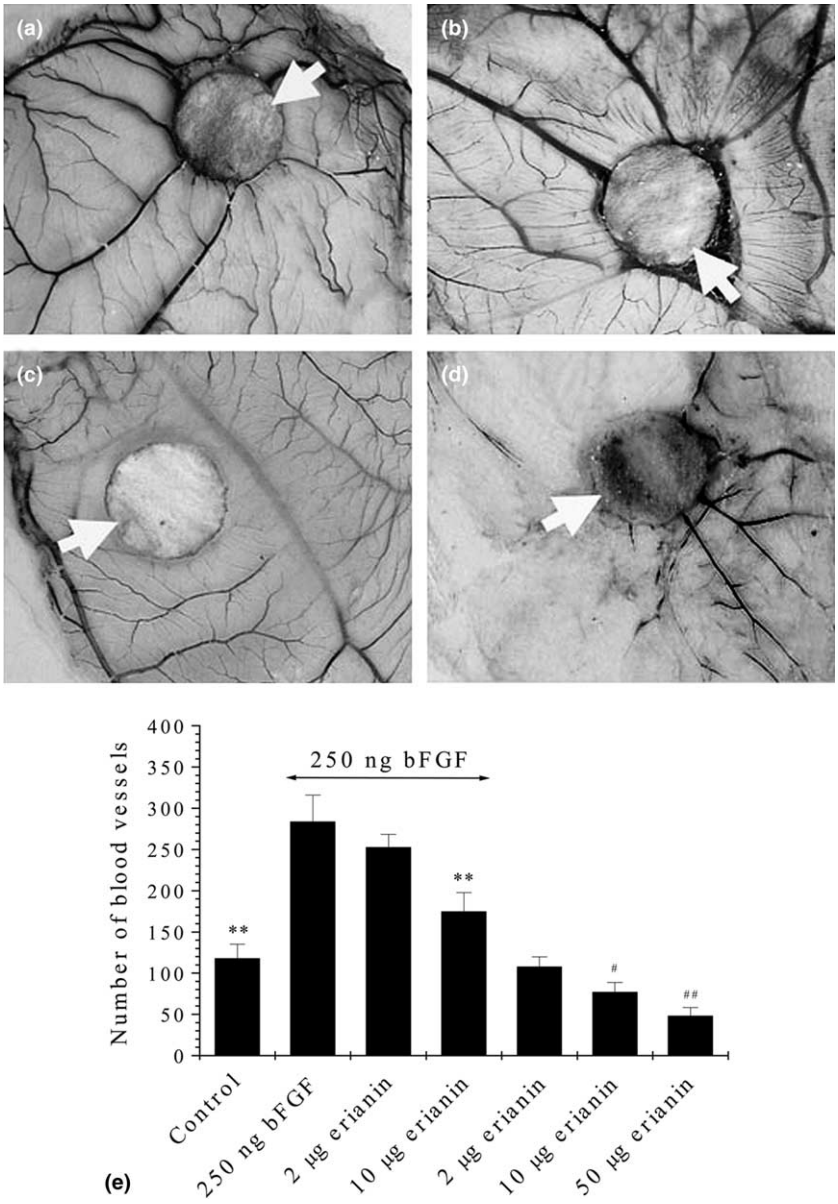

Fig. 4. Effect of erianin on neovascularisation of chick embryo. Blank filter discs and discs containing basic fibroblast growth factor (bFGF), bFGF plus erianin or erianin alone, placed on chick chorioallantoic membranes and incubated for 48 h. Representative images from (a) blank control, (b) 250 ng/egg bFGF, (c) 10 μg/egg erianin, and (d) 50 μg/egg erianin. Arrows indicate the filter discs. (e) Macroscopic assessment of vascular density conducted by counting the number of blood vessels within a 100 mm^2 area surrounding discs. Bars indicate means ± SEM from triplicate assays ($n = 8$–10 for each assay). $^{**}P < 0.01$ vs. bFGF treatment, and $^{\#}P < 0.05$, $^{\#\#}P < 0.01$ vs. control (Student's t-test).

dose-dependent anti-angiogenic effects: the number of vessels around the disc absorbed with 10 μg erianin was diminished (Fig. 4(c)), and very few vessels were detectable with 50 μg erianin treatment (Fig. 4(d)). Treatment with bFGF plus 2 or 10 μg erianin efficiently abrogated the bFGF-induced angiogenic response. A quantitation assay is shown in Fig. 4(e), indicating inhibitive actions of erianin against both bFGF-induced and spontaneous angiogenesis.

3.4. Erianin inhibits endothelial proliferation with selectivity

Erianin induced anti-proliferative responses in a concentration-dependent manner, with an EC_{50} of 34.1 ± 5.3 nM in normal HUVECs, in contrast to slight effects against A357 and NIH/3T3 cells at concentrations ranging from 10^{-9} to 10^{-6} M of erianin (Fig. 5(a)), which implies that erianin provided selective inhibition of proliferation toward endothelial cells. Moreover, treatment with erianin produced an enhanced effect against HUVECs in the presence of tumour-secreted factors, with an EC_{50} of 19.5 ± 3.6 nM ($P < 0.05$, vs. the EC_{50} of normal HUVECs, Student's *t*-test), and further studies on the effects of erianin on quiescent endothelium suggested that this selective inhibition was mainly directed toward proliferating endothelium (Fig. 5(b)). Furthermore, to validate these data from the MTT assay, which is affected by both the amount and the energy metabolism of cells, a cell-counting assay with crystal violet [27] was performed and similar data were obtained (not shown).

As a negative control, starvation of cells by omitting FBS abolished proliferation, as indicated by less absorbance on the MTT assay than with the complete

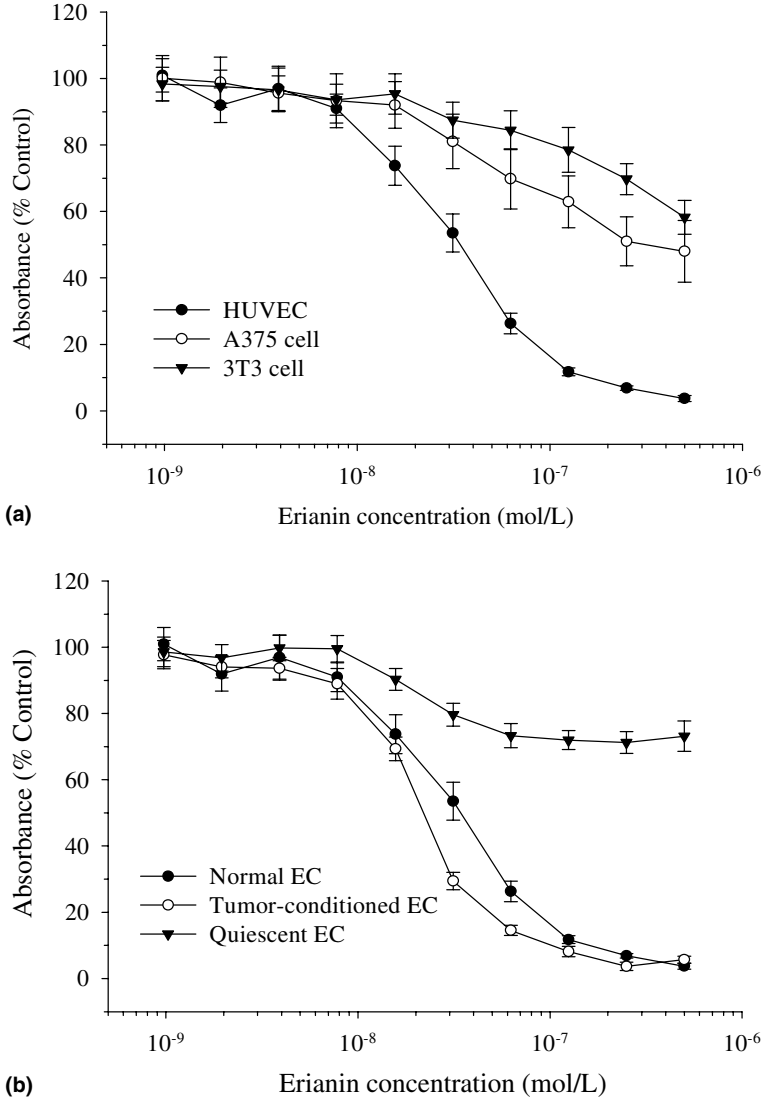

Fig. 5. The anti-proliferative profile of erianin against (a) normal endothelium vs. A375 and NIH/3T3 cells, (b) human umbilical vein endothelial cells (HUVEC) under different conditions. Cell proliferation was determined by MTT assay. Results are expressed as a percentage of control ± SEM from 4 to 6 assays (($n = 8$ for each assay).

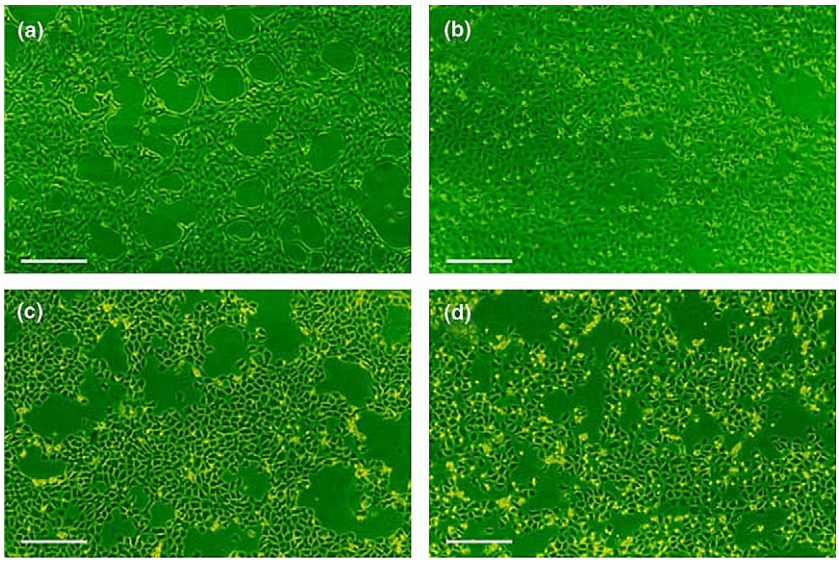

Fig. 6. Effect of erianin on human umbilical vein endothelial cells (HUVEC) tube formation. After subculture on collagen gels for 24 h, HUVECs were incubated (a) without or (b) with 10 nM erianin for 24 h, and established tube formation was treated with 10 nM erianin for (c) 3 h or (d) 12 h. Images representative of one experiment out of three ($n = 6$ for each assay). Bar = 250 μM.

medium of the positive control (35.8% ± 4.2% of positive control in HUVECs, 25.3% ± 2.9% in A357 cells, and 29.5% ± 3.6% in NIH/3T3 cells). On comparing these data for negative controls with the data shown in Fig. 5, it appears that erianin at doses of 1–50 nM mainly showed anti-proliferative activity rather than direct cytotoxicity in normal proliferating HUVECs. In addition, the non-cytotoxic concentration of erianin was established as 10 nM, one-third of EC_{50} in normal HUVECs, which was confirmed by LDH assay: 24-h treatment with 10 nM erianin failed to cause a significant increase in LDH release, 8.7 ± 2.41% of the total LDH for erianin incubation, compared with a blank control (5.5 ± 1.65%) ($n = 8$).

3.5. Erianin abolishes tube formation, migration and adhesion in HUVECs

When endothelial cells were subcultured on collagen for 48 h, tube formation was achieved (Fig. 6(a)) and there was not discernible tube structure in endothelial monolayers incubated with 10 nM erianin (Fig. 6(b)). The addition of DMEM containing erianin at this concentration to already established endothelial cell networks resulted in rapid disruption of these networks. Disruption started after approximately 3 h and was complete after 12 h of exposure to erianin (Fig. 6(c) and (d)). Endothelial migration and adhesion in response to a gradient of erianin was measured; erianin inhibited both the migration and adhesion of HUVECs, with a significant effect observed at 10 nM (Fig. 7).

3.6. Non-cytotoxic erianin disrupts endothelial cytoskeleton

HUVECs grown on coverslips had a normally distributed endothelial cytoskeleton (Figs. 8(a)–(c) and 9(a)–(c)). Incubation of proliferating HUVECs with non-cytotoxic 10 nM erianin for 1 h resulted in cytoskeletal disorganisation and disruption of both F-actin filaments and β-tubulin microtubules (Figs. 8(e) and (f), and 9(e) and (f), while at this dose of erianin, there was no obvious change in the appearance of confluent endothelium (Figs. 8(d) and 9(d)) and equivalent changes became noticeable only when increasing the concentration of erianin to 100 nM (data not shown). In addition, in parallel studies on other cells including A375, Bel7402, and NIH/3T3, treatment with 10 nM erianin failed to influence the cytoskeletal distribution of F-actin and β-tubulin (data not shown), implying that there is cell-type specificity in erianin-induced cytoskeletal impairment.

Further evidence was provided by transmission electron microscopy, as shown in Fig. 10. HUVECs cultured in DMEM appeared elongated, containing well-developed organelles and a network of microtubules and microfilaments extending across the cytoplasm and thickened near the subcortical plasma membrane (Fig. 10(a) and (b)). After exposure to10 nM erianin for 1 h, HUVECs displayed lesions of the cytoskeleton microfilaments in the form of perinuclear and subcortical areas of condensation and depolymerisation. Thickened but non-continuous and divided microfilaments were distributed in the cytoplasm and subcortex (Fig. 10(c)–(e)), and depolymerised microtubules were dispersed among organelles in erianin-treated HUVECs (Fig. 10(f)).

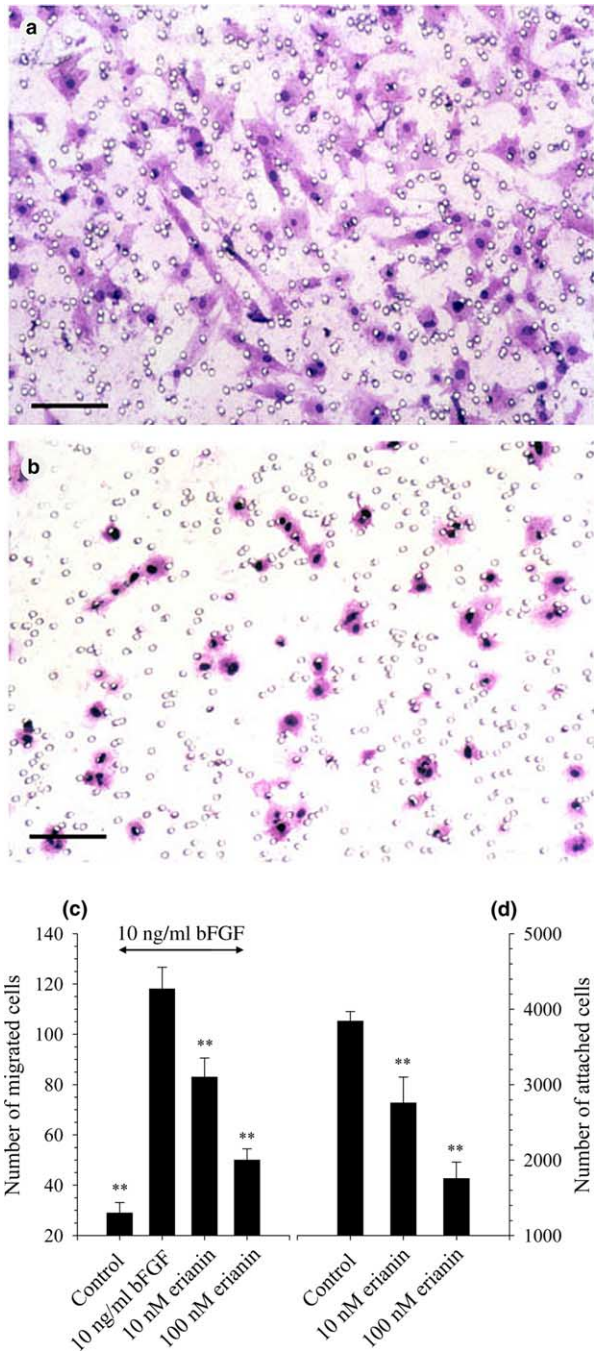

Fig. 7. Effect of erianin on migration and adhesion of human umbilical vein endothelial cells (HUVEC). (a–c) HUVECs seeded on Transwells were incubated with Dulbecco's modified Eagle's medium as control, 10 ng/ml basic fibroblast growth factor (bFGF) alone, and bFGF plus 10 or 100 nM erianin for 24 h. Migrated cells were fixed and stained, and representative images taken for migrated HUVECs exposed with (a) 10 ng/ml bFGF, or (b) 10 ng/ml bFGF plus 10 nM erianin. (c) Quantitative assay counting the average number of migrated cells per field (100× magnification). Traces indicate means ± SEM from triplicate assays ($(n = 5–6$ for each assay). $^{**}P < 0.01$ vs. bFGF treatment (Student's *t*-test). (d) Suspended HUVECs added to fibronectin-coated wells in the presence or absence of erianin and allowed to attach for 90 min. Adhesive cells were counted after crystal violet staining and data expressed as the number of attached cells per well. Traces indicate means ± SEM from triplicate assays ($n = 6–8$ for each assay). $^{**}P < 0.01$ vs. control (Student's *t*-test).

4. Discussion

In the present study, we addressed the anti-angiogenic activity of erianin *in vivo* and *in vitro*. *In vivo* activity was assessed in relation to two tumours representative of carcinoma and sarcoma, hepatoma Bel7402, and melanoma A375, respectively. The results showed that 100 mg/kg per day erianin induced a moderate growth delay in both tumours accompanied by obvious haemorrhagic necrosis. Other anti-angiogenic drugs or prodrugs, such as combretastatin A-4, are also reported to produce only a slight delay in tumour growth, or no measurable effect in some models, since tumours may continue to grow from the viable rim that is supplied by the normal tissue vasculature [30], but combination therapy with traditional chemotherapy agents induced increased activity [31,32]. One of the most important properties of angiogenesis inhibitors may to enhance the anti-tumour efficacy of conventional chemotherapy. In addition, erianin provided a more effective anti-tumour activity against A375 than that against Bel7402, as indicated by the more significant decrease in tumour weight and increase in TVD time in the A375 tumour. These differences very probably result from the fact that there is a more abundant vascular distribution in the A735 tumour than that in the Bel7402 (IMD of A735 is approximately 1.4 times greater than that of Bel7402), which also supports the notion that erianin exerts its anti-tumour effect via anti-angiogenesis.

Obvious and extensive haemorrhagic necrosis is observed in tumours after treatment with anti-angiogenic drugs, due to their direct toxicity toward abnormal vasculature. In present experiment, massive erianin-induced haemorrhage was clearly discernible at 2 h at a dose of 100 mg/kg (the dose that caused tumour growth delay with no obvious toxicity), followed by haemorrhagic necrosis at 4 and 24 h. That treatment with erianin-induced early, time-dependent necrosis in relation to tumoural vascular damage further indicates that this vascular shutdown might be directly responsible for the morphological changes. Furthermore, the anti-angiogenic activity of erianin was confirmed in a CAM assay *in vivo*, which demonstrated a potent inhibitive effect of erianin on spontaneous and bFGF-stimulated neovascularisation/angiogenesis in the chicken embryo.

Recently, strategies for anti-angiogenic drugs were described as follows: (1) inhibition of endothelial cell proliferation; (2) interference with endothelial cell adhesion and migration; (3) interference with metalloproteinases [33]. According to our present research, erianin directly interferes with endothelial behaviour, in agreement with our previous finding that erianin induces metabolic inhibition in HUVECs [17]. That erianin produced greater toxicity against endothelial cells than other cells shows a selective property of erianin. The

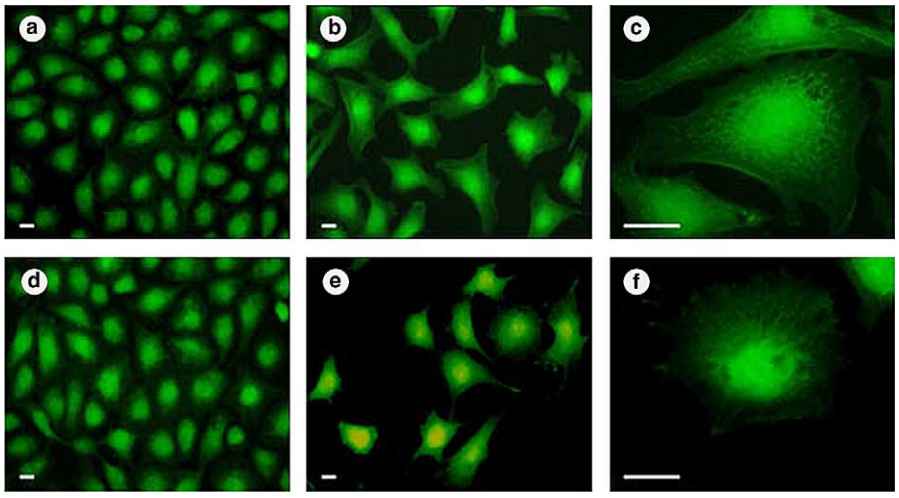

Fig. 8. Fluorescent microscopic images of F-actin. Confluent or proliferating human umbilical vein endothelial cells were incubated with Dulbecco's modified Eagle's medium in the presence or absence of 10 nM erianin for 1 h, and F-actin was visualised by fluorescent staining. (a) Control confluent cells; (b,c) control proliferating cells; (d) erianin-treated confluent cells; (e,f) erianin-treated proliferating cells. Images shown are representative of independent triplicate assays. Bar = 10 μM.

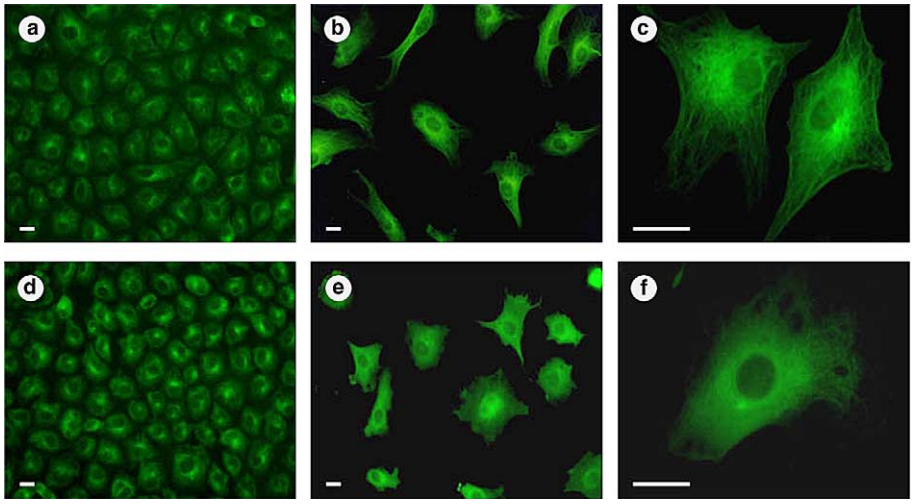

Fig. 9. Fluorescent microscopic images of β-tubulin. Confluent or proliferating human umbilical vein endothelial cells were incubated with Dulbecco's modified Eagle's medium in the presence or absence of 10 nM erianin for 1 h, and the β-tubulin visualised by fluorescent staining. (a) Control confluent cells; (b,c) control proliferating cells; (d) erianin-treated confluent cells; (e,f) erianin-treated proliferating cells. Images shown are representative of independent triplicate assays. Bar = 10 μM.

ideal anti-vascular agent might be able to exert potent effects on both tumour cells and vascular endothelial cells [34], but those agents so far tested often display a strong toxicity that limits the actual value of their clinic application. Generally, a reagent designed to target abnormal endothelium might be more valuable, despite a possibly incomplete anti-tumour effect with a single administration, if its advantages can be displayed with combination chemotherapy. In this report, the ability of erianin to inhibit endothelial tube formation, migration, and adhesion indicates that it might work at more than one step in the process of angiogenesis, or that its effect is common to tube formation, migration and adhesion, which may also constitute the basis of its anti-tumour activity.

The data presented here show that erianin not only has an anti-proliferative effect on endothelium with a cell-type specificity, but also that this effect is restricted to proliferating endothelial cells rather than quiescent/confluent cells, indicating that erianin holds a high selectivity as an anti-vascular agent. Since endothelial cells lining tumour vessels are proliferating between 20 and 2000 times as rapidly as normal endothelium [35], this selective sensitivity of erianin toward proliferating endothelium could contribute to its potential therapeutic applications. Moreover, similar results were obtained in

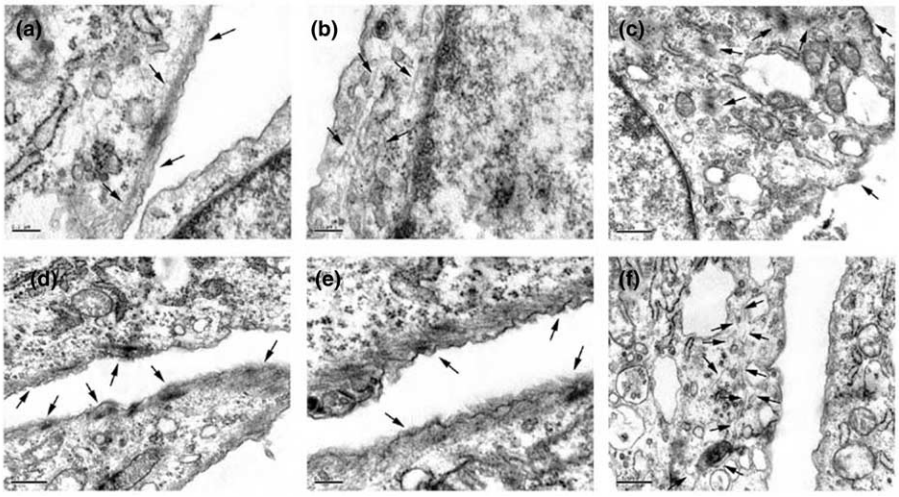

Fig. 10. Ultrastructure of human umbilical vein endothelial cells. (a,b) Control; (c–f) after 1-h exposure to 10 nM erianin. (a) Cells contain well-developed organelles and subcortical microfilaments (arrow) extend across them; (b) cells show normal distribution of cytoskeleton microtubules (arrow). After 1-h treatment with 10 nM erianin, thickened and discontinuous microfilaments (arrow) appear in cytoplasm (c) and subcortex (d,e,f) depolymerised microtubules (arrow) are seen among the organelles. Representative images taken from triplicate assays (a,b,e: bar = 0.2 μM; c,d,f: bar = 0.5 μM).

cytoskeletal studies: (1) non-cytotoxic erianin-induced cytoskeletal damage was endothelium selective, and is very likely to be the molecular basis of its anti-vascular/anti-angiogenic effects; (2) exposure to 10 nM erianin induced rapid and obvious disorganisation of both F-actin and β-tubulin in isolated endothelial cells, inclined to mitogenesis, rather than confluent ones, implying that direct disruption of the mitotic cytoskeleton might contribute to the selective cytotoxicity of erianin toward proliferating endothelium. Further detailed data were provided by transmission electron microscopy, which demonstrated that erianin could induce rapid cytoskeletal lesions in both microfilaments and microtubules in endothelial cells.

The proliferating cells had fewer microtubule-associated proteins (MAPs) [36], which will reduce microtubule dynamic instability [37], fewer post-translational tubulin modifications [38], and more isotype spectra in their tubulins [39], which might otherwise be the intracellular targets for the selective action of erianin in proliferating endothelium. While tubulin and actin are in very close association and once one of them is disturbed, the other will not remain unaffected and cannot maintain the cellular architecture, the possibility that actin filaments and their regulatory proteins, not tubulin, could be selectively targeted in cancer chemotherapy is very attractive [40]. Our present findings indicate that erianin also provides selective activity toward F-actin in proliferating HUVECs, the detailed molecular mechanism of which remains to be fully understood.

In summary, our current studies provide evidence for anti-angiogenic activities of erianin: it induced tumour vascular shutdown *in vivo*, inhibited angiogenesis in CAM, abrogated the proliferation of HUVECs, disrupted endothelial tube formation, and abolished cell migration and adhesion. Erianin disorganised the cytoskeleton at a non-cytotoxic dose. All of these findings hint that, as a novel anti-angiogenic agent, erianin might be a prototype anti-tumour drug.

Acknowledgements

This work was supported by a grant to Dr. Zheng-Tao Wang from the Shanghai Key Subject foundation, Science and Technology Development Found (No. 00XD14022). The authors gratefully acknowledge Dr. Jin-jun Li (National Laboratory for Oncogenes and Related Genes, Shanghai Cancer Institute, Shanghai, PR China) for excellent support and Professor Hui-Fang Pang (Department of Pathology, Shanghai University of Traditional Chinese Medicine, Shanghai) for helpful discussions.

References

1. Folkman J. Angiogenesis in cancer, vascular, rheumatoid and other disease. *Nat Med* 1995, **1**, 27–31.
2. Papetti M, Herman IM. Mechanisms of normal and tumour-derived angiogenesis. *Am J Physiol* 2002, **282**, C947–C970.
3. Fan TP, Jaggar R, Bicknell R. Controlling the vasculature: angiogenesis, anti-angiogenesis and vascular targeting of gene therapy. *Trends Pharmacol Sci* 1995, **16**, 57–66.
4. Ingber D, Fujita T, Kishimoto S, Sudo K, Kanamaru T, Brem H, *et al*. Synthetic analogues of fumagillin that inhibit angiogenesis and suppress tumour growth. *Nature* 1990, **348**, 555–557.
5. O'Reilly MS, Holmgren L, Shing Y, Chen C, Rosenthal RA, Moses M, *et al*. Angiostatin: a novel angiogenesis inhibitor that mediates the suppression of metastases by a Lewis lung carcinoma. *Cell* 1994, **79**, 315–328.

6. O'Reilly MS, Boehm T, Shing Y, Fukai N, Vasios G, Lane WS, *et al*. Endostatin: an endogenous inhibitor of angiogenesis and tumour growth. *Cell* 1997, **88**, 277–285.
7. Gingras D, Batist G, Beliveau R. AE-941 (Neovastat): a novel multifunctional antiangiogenic compound. *Expert Rev Anticancer Ther* 2001, **1**, 341–347.
8. Dark GG, Hill SA, Prise VE, Tozer GM, Pettit GR, Chaplin DJ. Combretastatin A-4, an agent that displays potent and selective toxicity toward tumour vasculature. *Cancer Res* 1997, **57**, 1829–1834.
9. Manfredi KP, Vallurupalli V, Demidova M, Kindscher K, Pannell LK. Isolation of an anti-HIV diprenylated bibenzyl from *Glycyrrhiza lepidota*. *Phytochemistry* 2001, **58**, 153–157.
10. Kamory E, Keseru GM, Papp B. Isolation and antibacterial activity of marchantin A, a cyclic bis (bibenzyl) constituent of Hungarian *Marchantia polymorpha*. *Planta Med* 1995, **61**, 387–388.
11. Dekanski JB. Anti-prostatic activity of bifluranol, a fluorinated bibenzyl. *Br J Pharmacol* 1980, **71**, 11–16.
12. Cushman M, Nagarathnam D, Gopal D, Chakraborti AK, Lin CM, Hamel E. Synthesis and evaluation of stilbene and dihydrostilbene derivatives as potential anticancer agents that inhibit tubulin polymerization. *J Med Chem* 1991, **34**, 2579–2588.
13. Lee YHR, Park JD, Baek NI, Kim SI, Ahn BZ. In vitro and in vivo antitumoural phenanthrenes from the aerial parts of *Dendrobium nobile*. *Planta Med* 1995, **61**, 178–180.
14. Ma GX, Xu GJ, Xu LS. Inhibitory effects of *Dendrobium chrysotoxum* and its constituents on the mouse HePA and ESC. *J Chin Pharmaceut Univ* 1994, **25**, 188–189.
15. Ma GX, LeBlanc GA. The activity of erianin and chrysotoxine from *Dendrobium chrysotoxum* to reverse multidrug resistance in B16/h MDR-1 cells. *J Chin Pharmaceut Sci* 1998, **7**, 142–146.
16. Li YM, Wang H, Liu GQ. Erianin induces apoptosis in human leukemia HL-60 cells. *Acta Pharmacol Sin* 2001, **22**, 1018–1022.
17. Gong YQ, Fan Y, Liu L, Wu DZ, Chang ZL, Wang ZT. Erianin induces a JNK/SAPK-dependent metabolic inhibition in human umbilical vein endothelial cells. *In vivo* 2004, **18**, 223–228 .
18. Ng TB, Liu F, Wang ZT. Antioxidative activity of natural products from plants. *Life Sci* 2000, **66**, 709–723.
19. Tomayko MM, Reynolds CP. Determination of subcutaneous tumour size in athymic (nude) mice. *Cancer Chemother Pharmacol* 1989, **24**, 148–154.
20. Smith KA, Hill SA, Begg AC, Denekamp J. Validation of the fluorescent dye Hoechst 33342 as a vascular space marker in tumours. *Br J Cancer* 1988, **57**, 247–253.
21. Blebea J, Vu JHR, Assadnia S, McLaughlin PJ, Atnip RG, Zagon IS. Differential effects of vascular growth factors on arterial and venous angiogenesis. *J Vasc Surg* 2002, **35**, 532–538.
22. Fan Y, Wu DZ, Gong YQ, Xu R, Hu ZB. Metabolic responses induced by thrombin in human umbilical vein endothelial cells. *Biochem Biophys Res Commun* 2002, **293**, 979–985.
23. Carmichael J, DeGraff WG, Gazdar AF, Minna JD, Mitchell JB. Evaluation of a tetrazolium-based semiautomated colorimetric assay: assessment of chemosensitivity testing. *Cancer Res* 1987, **47**, 936–942.
24. Decker T, Lohmann-Matthes ML. A quick and simple method for the quantitation of lactate dehydrogenase release in measurements of cellular cytotoxicity and tumour necrosis factor (TNF) activity. *J Immunol Methods* 1988, **115**, 61–69.
25. Fan Y, Wu DZ, Gong YQ, Zhou JY, Hu ZB. Effects of calycosin on the impairment of barrier function induced by hypoxia in human umbilical vein endothelial cells. *Eur J Pharmacol* 2003, **481**, 33–40.
26. Wang F, Van Brocklyn JR, Hobson JP, Movafagh S, Zukowska-Grojec Z, Milstien S, *et al*. Sphingosine 1-phosphate stimulates cell migration through a G_i-coupled cell surface receptor. *J Biol Chem* 1999, **274**, 35343–35350.
27. Nie D, Hillman GG, Geddes T, Tang K, Pierson C, Grignon DJ, *et al*. Platelet-type 12-lipoxygenase in a human prostate carcinoma stimulates angiogenesis and tumour growth. *Cancer Res* 1998, **58**, 4047–4051.
28. Vacca A, Iurlaro M, Ribatti D, Minischetti M, Nico B, Ria R, *et al*. Antiangiogenesis is produced by nontoxic doses of vinblastine. *Blood* 1999, **94**, 4143–4155.
29. Wulf E, Deboben A, Bautz FA, Faulstich H, Wieland T. Fluorescent phallotoxin, a tool for the visualization of cellular actin. *Proc Natl Acad Sci USA* 1979, **76**, 4498–4502.
30. Grosios K, Loadman PM, Swanine DJ, Pettit GR, Bibby MC. Combination chemotherapy with combretastatin A4 phosphate and 5-fluorouracil in an experimental murine colon adenocarcinoma. *Anticancer Res* 2000, **20**, 229–234.
31. Chaplin DJ, Pettit GR, Hill SA. Anti-vascular approaches to solid tumour therapy: evaluation of combretastatin A4 phosphate. *Anticancer Res* 1999, **19**, 189–196.
32. Sweeney CJ, Miller KD, Sledge Jr GW. Resistance in the anti-angiogenic era: nay-saying or a word of caution. *Trends Mol Med* 2003, **9**, 24–29.
33. Griffioen AW, Molema G. Angiogenesis: potentials for pharmacologic intervention in the treatment of cancer, cardiovascular diseases, and chronic inflammation. *Pharmacol Rev* 2000, **52**, 237–268.
34. Hill SA, Sampson LE, Chaplin DJ. Anti-vascular approaches to solid tumour therapy: evaluation of vinblstine and flavone acetic acid. *Int J Cancer* 1995, **63**, 119–123.
35. Denekamp J, Hobson B. Endothelial-cell proliferation in experimental tumours. *Br J Cancer* 1982, **46**, 711–720.
36. Mandelkow E, Manderlkow EM. Microtubules and microtubule-associated proteins. *Curr Opin Cell Biol* 1995, **7**, 72–81.
37. Maccioni RB, Cambiazo V. Role of microtubule-associated proteins in the control of microtubule assembly. *Physiol Rev* 1995, **75**, 835–864.
38. Tint IS, Bershadky AD, Gelfand IM, Vasiliev JM. Post-translational modification of microtubules is a component of synergic alterations of cytoskeleton leading to formation of cytoplasmic processes in fibroblasts. *Proc Natl Acad Sci USA* 1991, **88**, 6319–6322.
39. Dumontet C, Durian GE, Steger KA, Murphy GL, Sussman H, Stikic BL. Differential expression of tubulin isotypes during the cell cycle. *Cell Motil Cytoskeleton* 1996, **36**, 49–58.
40. Jordan MA, Wilson L. Microtubules and actin filaments: dynamic targets for cancer chemotherapy. *Curr Opin Cell Biol* 1998, **10**, 123–130.